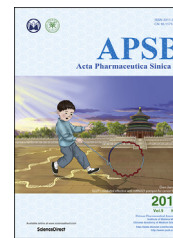




Chinese Pharmaceutical Association
Institute of Materia Medica, Chinese Academy of Medical Sciences

Acta Pharmaceutica Sinica B

www.elsevier.com/locate/apsb
www.sciencedirect.com



REVIEW

Red blood cell membrane-camouflaged nanoparticles: a novel drug delivery system for antitumor application



Qing Xia[†], Yongtai Zhang[†], Zhe Li, Xuefeng Hou, Nianping Feng^{*}

Department of Pharmaceutical Sciences, Shanghai University of Traditional Chinese Medicine, Shanghai 201203, China

Received 15 September 2018; received in revised form 30 October 2018; accepted 28 November 2018

KEY WORDS

Red blood cells;
Membrane;
Nanoparticles;
Drug delivery;
Antitumor;
Biomimetic nanoparticles

Abstract Erythrocytes (red blood cells, RBCs) are the most abundant circulating cells in the blood and have been widely used in drug delivery systems (DDS) because of their features of biocompatibility, biodegradability, and long circulating half-life. Accordingly, a “camouflage” comprised of erythrocyte membranes renders nanoparticles as a platform that combines the advantages of native erythrocyte membranes with those of nanomaterials. Following injection into the blood of animal models, the coated nanoparticles imitate RBCs and interact with the surroundings to achieve long-term circulation. In this review, the biomimetic platform of erythrocyte membrane-coated nano-cores is described with regard to various aspects, with particular focus placed on the coating mechanism, preparation methods, verification methods, and the latest anti-tumor applications. Finally, further functional modifications of the erythrocyte membranes and attempts to fuse the surface properties of multiple cell membranes are discussed, providing a foundation to stimulate extensive research into multifunctional nano-biomimetic systems.

Abbreviations: ABC, accelerated blood clearance; APCs, antigen presenting cells; AuNCs, gold nanocages; AuNPs, gold nanoparticles; C8bp, C8 binding protein; CR1, complement receptor 1; DAF, decay accelerating factor; DDS, drug delivery systems; DLS, dynamic light scattering; Dox, doxorubicin; ECM, extracellular matrix; EpCam, epithelial cell adhesion molecule; EPR, enhanced permeability and retention; ETA, endothelin A; FA, folic acid; GA, gambogic acid; H&E, hematoxylin and eosin; HRP, homologous restriction protein; MCP, membrane cofactor protein; MNCs, magnetic nanoclusters; MNs, magnetic nanoparticles; MPS, mononuclear phagocyte system; MRI, magnetic resonance imaging; MSNs, mesoporous silica nanoparticles; NIR, near-infrared radiation; PAI, photoacoustic imaging; PBS, phosphate buffered saline; PCL, poly(caprolactone); PDT, photodynamic therapy; PEG, polyethylene glycol; PFCs, perfluorocarbons; PLA, poly(lactide acid); PLGA, poly(D,L-lactide-co-glycolide); PPy, polypyrrole; PS, photosensitizers; PTT, photothermal therapy; PTX, paclitaxel; RBCM-NPs, RBCM-coated nanoparticles; RBCMs, RBC membranes; RBCs, red blood cells; RES, reticuloendothelial system; rHuPH20, recombinant hyaluronidase, PH20; ROS, reactive oxygen species; RVs, RBCM-derived vesicles; SEM, scanning electron microscopy; SIRP α , signal-regulatory protein alpha; TEM, transmission electron microscopy; TEMPO, 2,2,6,6-tetramethylpiperidin-1-yl oxiyl; TPP, triphenylphosphonium; UCNPs, upconversion nanoparticles; UV, ultraviolet

^{*}Corresponding author.

E-mail address: npfeng@shutcm.edu.cn (Nianping Feng).

[†]These authors made equal contributions to this work.

Peer review under responsibility of Institute of Materia Medica, Chinese Academy of Medical Sciences and Chinese Pharmaceutical Association.

<https://doi.org/10.1016/j.apsb.2019.01.011>

2211-3835 © 2019 Chinese Pharmaceutical Association and Institute of Materia Medica, Chinese Academy of Medical Sciences. Production and hosting by Elsevier B.V. This is an open access article under the CC BY-NC-ND license (<http://creativecommons.org/licenses/by-nc-nd/4.0/>).

1. Introduction

Over previous decades, nanoparticle-based drug delivery systems (DDS) have been successfully applied experimentally and clinically to improve the efficacy of many drugs and therapeutic molecules^{1,2}. Such DDSs can achieve passive tumor targeting owing to the enhanced permeability and retention (EPR) effect^{3,4}. Compared to the free-drug, nanoparticle-based drugs are characterized by low toxicity, good stability, outstanding biocompatibility, higher drug release efficiency, higher blood retention time, and long shelf-life for biomedical applications⁵. However, especially for cancer treatments, ideal nanoparticles should also possess features of extended blood circulation, tumor tissue targeting, and cancer cell binding.

Therapeutic molecules are often released early or captured by the immune system *in vivo*; however, compensation by increasing drug dosage may not be a viable option as overdosage often results in unexpected side effects in normal tissues. Therefore, polyethylene glycol (PEG) functionalization has been widely used in various nanocarriers, as this can effectively avoid phagocytosis through the mononuclear phagocyte system (MPS) to achieve long-term circulation in the body. The principle is that these hydrophilic polymers hide the nanoparticles behind a hydration layer to reduce their immune clearance⁶, resulting in a modified nanoparticle half-life of several tens of hours whereas that of nonPEGylated nanoparticles is only a few minutes⁷. However, the appearance of anti-PEG immune responses in some patients has shifted research focus to the new field of bio-inspired nanocarriers. These novel biomimetic strategies commonly utilize features that imitate the body's internal components, and mimicking many natural mechanisms to achieve targeted effects^{8–12}.

Various kinds of cell membranes have been inspired from nature to realize long-term circulation or tumor targeting including membranes from cancer cells, bacteria, lymphocytes, platelets, leukocytes, and erythrocytes (red blood cells, RBCs). Affording blood circulation up to 120 days, RBCs were studied initially and have been used as an ideal carrier to deliver various bioactive compounds, such as enzymes, drugs, proteins, and macromolecules¹³. Moreover, mature RBCs lack a nucleus and various organelles, which is very favorable for their extraction and purification¹⁴. As the most abundant cells in the human body, human blood contains 5 billion RBCs per milliliter on average, providing rich coating materials for drug carrier functionalization. RBCs constitute biconcave discs averaging 7.8- μm diameter, 2.5- μm edge and 1- μm center thickness, and 85–91 fl (μm^3) volume¹⁵. Upon decreased osmotic pressure of the surrounding medium, RBCs become cupular and eventually spherical¹⁵. This swelling feature is a key to the feasibility of loading RBCs with drugs or other chemicals. In summary, the advantages of RBCs as carriers to load nanoparticles include^{15–17}: a) escaping the immune system and achieving long-term circulation; b) marked inherent biocompatibility and biodegradability; c) avoiding some intrinsic nano-preparation toxicities; d) lifespan up to 120 days; e) readily achieving high load capacity owing to the large quantities of cell membranes; and f) improving nanoparticle stability, enhancing *in vitro* storage time, and discouraging aggregation.

Notably, erythrocyte membrane-coated nano-formulations have been widely adopted in antitumor research to considerable achievement^{18–20}. Some properties of RBCs, such as structure and surface proteins, have also been utilized as design clues to devise the next generation of drug delivery platforms^{21–23}. In this review, we narrow our focus to various aspects of the field of erythrocyte membrane-coated nano-cores, particularly emphasizing coating mechanisms, preparation methods, verification methods, and the latest anti-tumor applications. Current advances provide confidence toward their clinical application in the near future. However, because this platform is composed of biological materials, strict disinfection and rigorous blood group matching are required to maximize compatibility and avoid the risk of immunogenicity.

2. History of erythrocytes as drug carriers

RBCs were first described in human blood samples in the 17th century by Dutch scientist Lee Van Hock, with their flat disc rather than spherical shape identified after another century by Howson. In 1953, Gardos attempted to load the “erythrocyte ghosts” with ATP, with this attempt laying the foundation for subsequent coating of the erythrocyte membrane with various active ingredients, opening up a whole new area of drug delivery strategies. In 1959, Marsden and Ostling²⁴ reported the entrapment of dextrans in erythrocytes, followed by the use of RBC loading with therapeutic agents for delivery purposes by Ihler et al.¹³. Subsequently, the term “carrier red blood cells” was introduced in 1979²⁵.

Following a groundbreaking study of the treatment of Gaucher's disease with β -glucosidase and β -galactosidase using carrier erythrocytes in the 1970s¹³, many enzyme replacement therapeutic methodologies have been developed, such as gentamicin, daunorubicin, and L-asparaginase loading into erythrocytes for respectively treating bacterial infections, leukemia, and asparagine-dependent leukemia²⁶. In 1994, Lejeune et al.²⁷ reported the preparation of RBC membrane-derived liposomes, also termed “nanoerythroosomes”, which was obtained by physically squeezing RBC ghosts through membranes with defined pore sizes. However, simply conjugating active molecules onto the surface of erythrocytes has been found to trigger a rapid clearance from the bloodstream, in addition to a tendency to cause vesicle aggregation, indicating that these erythrocyte ghosts lacking structural integrity are highly unstable²⁸. In 2013, the Zhang's group²⁹ proposed the definition of nanosponges, providing a biomimetic toxin nanosponge that functioned as a toxin decoy *in vivo*. Composed of polymer nanoparticle cores and surrounding erythrocyte membranes, the nanosponges could absorb membrane-damaging toxins, then transfer them away from the cell targets. Considered as one of the most exciting breakthroughs in this field, this work instigated a boom of bionic nano-medicine research (Fig. 1).

3. Immune escape mechanism of RBC membranes (RBCMs)

The long-term circulatory effect of erythrocytes is mediated by a series of membrane proteins on the membranes surface. Among these, CD47 constitutes an integral membrane protein with five

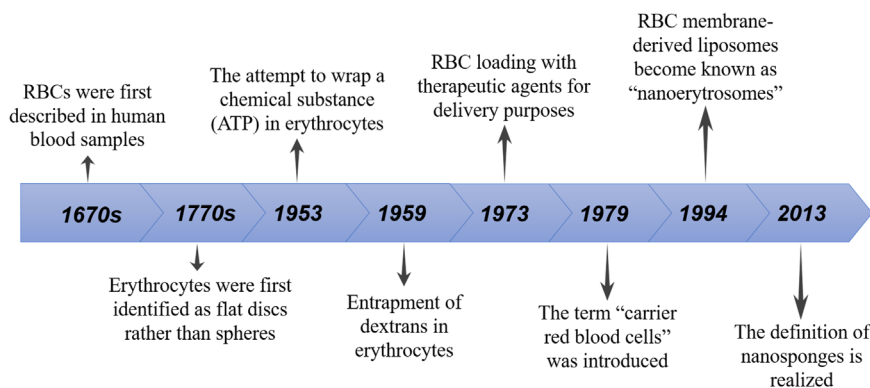


Figure 1 The historical process of RBCs as drug carriers.

membrane-spanning regions, firmly embedding it in RBCMs, along with an IgV-like extracellular domain that contributes to RBCM survival in circulation³⁰. CD47 also serves as a self-marker that can actively signal macrophages to prevent erythrocyte uptake³¹. Specifically, the signal-regulatory protein alpha (SIRP α) glycoprotein, which is expressed by phagocytic cells, interacts with and recognizes CD47 as a “do not eat me” signal, thereby inhibiting immune cell engulfment of RBCs^{32,33}.

Other membrane proteins such as C8 binding protein (C8bp), homologous restriction protein (HRP), decay accelerating factor (DAF), membrane cofactor protein (MCP), and complement receptor 1 (CR1) and CD59 on the surface of RBCMs also play a role in the defense of complement system attacks^{26,34–37}. Thus, these RBCM surface proteins can reduce the immune response by presenting drug nanocarriers as “self” to achieve long-term systemic circulation. Compared to PEGylated nanoparticles with half-lives of 15.8 h, RBCM-coated nanoparticles (RBCM-NPs) exhibit a half elimination of 39.6 h, an over two-fold improvement³⁸. These data demonstrated that the RBCM coating improves the circulation time and reduces the uptake of RBCM-NPs by the reticuloendothelial system (RES), thereby increasing the chances of nanoparticles entering the tumor through the EPR effect.

4. Preparation methods of RBCM-NPs

Various methods including physical and chemical property-based techniques have been reported for encapsulating drugs or other bioactive agents in erythrocytes, such as hypotonic hemolysis^{39,40}, hypotonic dilution^{41,42}, hypotonic dialysis⁴³, hypotonic preswelling^{44,45}, and osmotic pulse⁴⁶ or chemical perturbation of the membrane^{47,48} along with electrical breakdown⁴⁹. In addition, endocytosis, lipid fusion, and intrinsic uptake of substances by erythrocytes are used to encapsulate different compounds¹⁵. To achieve successful covering, the encapsulated compounds may require a considerable degree of water solubility as well as erythrocyte inactivity; *i.e.*, lack of physical and chemical interactions with erythrocyte membranes to avoid leakage from the loaded RBCs, which could result in toxicological problems. Therefore, drugs are commonly prepared into a nano-preparation with less toxicity and higher stability as the core, followed by the use of RBCMs to disguise the nano-preparations to avoid identification by immune systems.

4.1. Preparation of RBCM-derived vesicles (RVs)

In general, the optimized and common preparation of RBCM-NPs can be divided into two parts: membrane-derived vesicles from RBCs and

vesicle-particle fusion^{44,48,50}. RVs are obtained by combining two steps, hypotonic treatment and sequential extrusion. Fresh whole blood obtained from the organism (*e.g.*, mouse) is centrifuged at 4 °C to maintain protein activity, and then the serum and buffy coat are removed to collect erythrocytes. The resulting RBCs are repeatedly washed with phosphate buffered saline (PBS) and re-collected by centrifugation to remove residual plasma and other unwanted cells. RBC ghosts are then acquired by hypotonic treatment, wherein the washed RBCs are gently mixed with an excess of 0.25 \times PBS⁵⁰ and held to release the intracellular RBC components. Following high-speed centrifugation to remove hemoglobin, the RBC ghosts comprising the resulting pink precipitate are sonicated in a bath sonicator, and then passed through different pore size polycarbonate porous membranes using an Avanti mini-extruder to obtain the target size of RVs (Fig. 2). To keep the membrane bio-active, protease inhibitors are usually added to the samples and the samples are stored at 4 °C^{51–53}.

4.2. Coating mechanism of RBCM-NPs

The highly flexible RBC structure depends on the cell membrane viscoelasticity, cell content viscosity, and cell surface to volume ratio, which allow RBCs to pass through fairly narrow capillary networks and “sieving organs” such as the spleen and the liver³⁷. The dense polysaccharide coating on the RBC surface, termed glycocalyx, is important to cell stability and immune escape characteristics^{54,55}. These complex polysaccharides on the cell surface are equivalent to a hydrophilic coating for achieving spatial stability^{56,57}. Polymeric nanoparticles with higher surface energies are more likely to interact with the stabilized membranes of the polysaccharide to minimize total energy, whereas the stabilized RBCM-NP surface can effectively exclude further membrane interactions⁵⁸. This stabilization mechanism ensures the occurrence of monolayer film coating, even in the presence of excess RBCMs.

Additionally, the negatively charged sialyl residues in the polysaccharide terminal confer a charged asymmetry on the cell membranes that plays a key role in the interfacial interactions between RBCMs and nanoparticles. Analysis of positively and negatively charged nanoparticles coated with RBCMs by Luk et al.⁵⁸ demonstrated that negatively charged nanoparticles could form nuclei-shells with distinct particles, whereas positively charged nanoparticles only formed polydisperse aggregates (Fig. 3). These results could be attributed to the dense negatively charged sialic acid moiety of the outer membrane side, with the strong affinity from positively charged nanoparticles likely collapsing the lipid bilayer and hindering the local arrangement necessary for lipid coverage. In contrast, the negatively charged

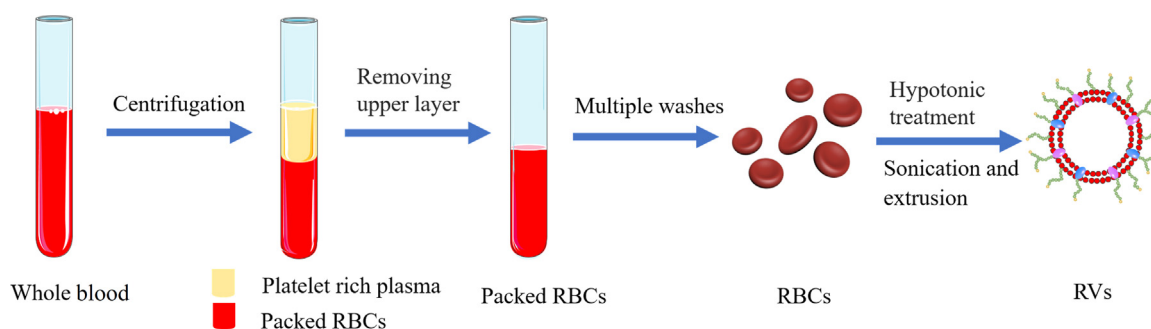


Figure 2 Schematic preparation of red blood cell membrane-derived vesicles (RVs). Fresh whole blood was centrifuged and repeatedly washed to obtain clean RBCs, and then RVs were obtained through further hypotonic and extrusion treatment.

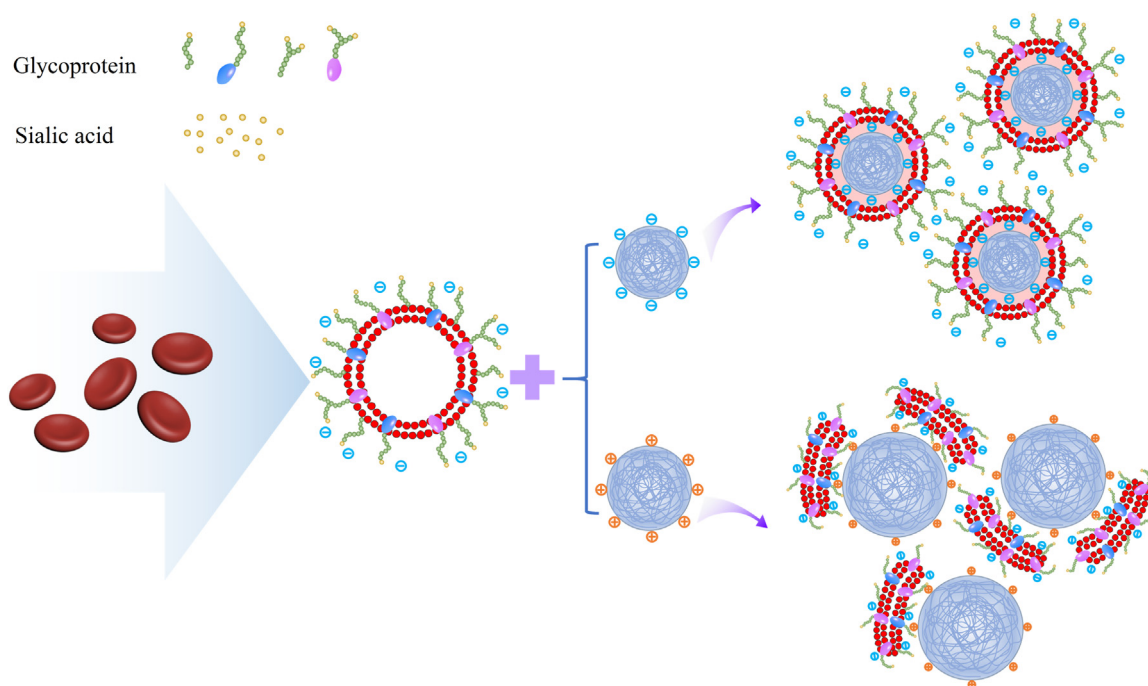


Figure 3 Schematic diagram of electrostatic interactions between negatively and asymmetrically charged RVs with negatively and positively charged polymeric cores, respectively. The negatively charged nanoparticles and the negatively charged RVs produce strong electrostatic repulsion, resulting in the fusion of the nanoparticles with the intracellular membrane side, while the positively charged nanoparticles and the negatively charged RVs produce a strong affinity to collapse the lipid bilayer. Adapted with permission from Ref. 58. Copyright © 2014 Royal Society of Chemistry.

nanoparticles and sialic acid moiety produced a strong electrostatic repulsion that caused the nanoparticles to fuse with the intracellular membrane side, forming a right-side-out-membrane orientation structure⁵⁹ to retain cell surface glycofocalyx.

4.3. Methods of vesicle-particle fusion

Early efforts devoted to bridging nanoparticles and RBCMs involved the use of “bottom-up” approaches, *i.e.* functionalizing nanoparticles with the surface chemistry of RBCs. However, the RBC-mimicking delivery vehicles formed by chemistry-based bioconjugation techniques often result in protein denaturation. Besides, the nanoparticles could hardly be adequately duplicated into a complex protein to anchor RBCMs. In 2011, Zhang et al.³⁸ reported a “top-down” method for producing RBCM-camouflaged nanoparticles. By extruding nanoparticles with nanoscale RVs

prepared in advance, they successfully coated the sub-100-nm PLGA nanoparticles with the RBCMs. This “top-down” method is promising for a large-scale production of RBCM-NPs. Herein, several main methods for RV-nanoparticle fusion are summarized.

4.3.1. Co-extrusion method

Prepared nanoparticles are usually fused with obtained RVs through mechanical extrusion. The principle for the coating process is the interfacial interactions mentioned above. Depending on the prepared nanoparticle size, the mixture is repeatedly extruded through different-sized porous membranes before bath sonication for several minutes⁵⁸ (Fig. 4A). The mechanical force promotes the nanoparticles to pass through the lipid bilayer, generating the vesicle-particle fusion. In particular, the RBCM phospholipid bilayer structure should be as complete as possible throughout the preparation process to minimize membrane protein

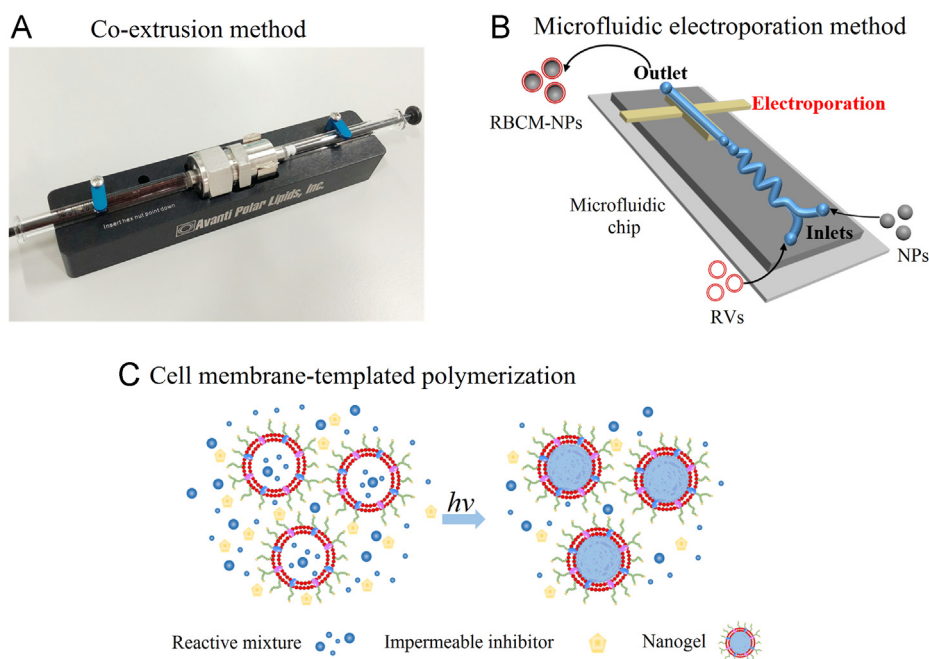


Figure 4 Schematic of RBCM-NP preparation by three different methods. (A) Co-extrusion method; (B) microfluidic electroporation method; Adapted with permission from Ref. 60. Copyright © 2017 American Chemical Society. (C) cell membrane-templated polymerization. Adapted with permission from Ref. 62. Copyright © 2015 Wiley Online Library.

loss and damage³⁸. After repeated extrusions, the excess vesicles are removed by centrifugation, with the collected precipitate representing the final product and redispersed for future use⁵⁰.

The ratio of the amount of RBCMs to nanoparticles is based on RBC membrane volume and the total membrane volume required to completely coat 1 mg of nanoparticles^{38,58}. Brian et al.⁵⁸ used different sizes of PLGA nanoparticles with diameters between 65 and 340 nm and coated by erythrocyte membranes, which resulted in different amounts of erythrocyte membranes as required. For the same weight of nanoparticles, the smaller the particle size, the fewer the red blood cell membranes needed. To compensate for cell membrane loss during preparation and the fusion process with nanoparticles, excessive amounts of blood are usually used to ensure that all nanoparticles are coated with RBCMs.

4.3.2. Microfluidic electroporation method

With the widespread use of biomimetic membrane-coated nanoparticles in the biomedical field, microfluidic electroporation has also been demonstrated to effectively promote RBCM-NP synthesis. Rao et al.⁶⁰ mixed Fe₃O₄ magnetic nanoparticles (MNs) and RVs in a microfluidic device. The microfluidic chip for electroporation consists of five sections: two inlets for the RVs and nanoparticles, respectively, a Y-shaped merging channel, an S-shaped mixing channel, an electroporation zone, and an outlet. When the mixture of MNs and RVs flows through the electroporation zone, the electrical pulses can break down the dielectric layer on the cell membranes and create multiple transient pores⁶¹, providing a pathway for the entry of Fe₃O₄ MNs. During this process, pulse voltage, duration, and flow rate should be optimized. After integration, the RBCM-MN are collected from the chips and injected into experimental animals for a series of *in vivo* performance tests (Fig. 4B).

The microfluidic electroporation strategy perfectly combines biology with physics, excluding the requirement of a very large

force to repeatedly squeeze the nanoparticles through porous membranes compared with the co-extrusion method, maintaining the membrane integrity to some extent and reducing cell surface protein loss, to achieve a better therapeutic effect. In addition, RBCM-MNs prepared by microfluidic electroporation exhibit better colloidal stability and magnetic resonance imaging (MRI) and photothermal therapy (PTT) performance *in vivo* than those prepared by conventional extrusion methods. Thus, the utilization of the microfluidic electroporation method in bio-inspired cell membrane coating of nanoparticles appears to have bright prospects.

4.3.3. Cell membrane-templated polymerization

The majority of existing cell membranes covering nanoparticles are prepared via a nanoparticle-templated coating routes, such as the co-extrusion method and microfluidic electroporation method, wherein the nanoparticle core is pre-synthesized then the outer layer coated with cell membranes. In this process, the interfacial interactions⁵⁸ between the membranes and the cores may hinder the application of some non-compliant nanomaterials. This led us to ponder the possibility of nanoparticle cores being grown *in situ* in cell-derived vesicles. Zhang et al.⁶² successfully implemented the first example of using a cell membrane-template polymerization method to synthesize polymer cores by *in situ* polymerization to form cell membrane-coated nanogels. They used acrylate polymerization as a model system, with the key to the study being the addition of a membrane-impermeable macromolecular inhibitor during membrane-templated formation, which was formed by the combination of a popular membrane-permeable free radical scavenger, 2,2,6,6-tetramethylpiperidin-1-yl oxyl (TEMPO), and PEG. The macromolecular inhibitor could effectively inhibit extracellular aggregation while maintaining the internal response of the vesicles, and reduce the risk of cell membrane protein denaturation and content leakage⁶². After the addition of the

macromolecular inhibitor, ultraviolet (UV) irradiation induced gelation, resulting in the formation of cell membrane-coated hydrogels, termed nanogels (Fig. 4C).

This method offers many advantages over the nanoparticle-templated coating route, including complete coating of the nanocores and easy control of the final biomimetic nanoparticle size and stiffness. Moreover, it overcomes the limitation requiring nanoparticles to be coatable, and provides a unique platform for a wide range of biomedical applications. Thus, the cell membrane-template method will likely be applicable to coating various nanostructures aside from nanogels.

5. *In vitro* verification of RBCM-NPs

In vitro evaluation of these cellular vectors is necessary as the chemical structures and surface proteins of the RBCMs play a vital role in their immune escape and circulation. The main characterization parameters are as follows.

5.1. Surface morphology

Nanoparticle size and potential values before and after RV encapsulation were examined using dynamic light scattering (DLS) measurement. The diameter of the coated nanoparticles is usually increased within the range of 10–20 nm, as the cell membrane lipid bilayer thickness is about 8 nm. The surface charge is close to the RVs after surface covering^{50,63,64}. In addition, a stabilizing effect on the RBCM-NPs in comparison with the naked nanoparticles has been demonstrated³⁷. Transmission (TEM) and scanning (SEM) electron microscopy are usually used to observe RV, nanoparticle, and RBCM-NP shape and morphology. Upon repeated extrusion, the original irregular cell membrane fragments are extruded into 100–200 nm hollow spherical vesicles, which differ completely from untreated RBC morphology, comprising a micron-level concave disc under electron microscopy. The hollow spherical vesicles also provide sufficient space for further nanoparticle encapsulation. Successful nanoparticle coating after negative staining can clearly be observed as a layer of membrane coated on the nanoparticle surface (*i.e.*, the core-shell structure) upon TEM visualization^{38,53,58,59}.

5.2. Verifications of surface proteins

Another proof of successful coating is the determination of whether the encapsulated nanoparticles carry the specific RBCM proteins, which determine whether the coated nanoparticles will have immune escape and long-term circulatory effects. Sodium dodecyl sulfate-polyacrylamide gel electrophoresis followed by Coomassie staining is used to visualize the RBC, RV, and RBCM-NP proteins, wherein all protein bands should show a similar profile to that of the RBCs^{53,59}. To further analyze specific protein markers, western blotting analysis is performed. CD235a, also known as glycoprotein A⁶⁵, the main RBC sialic acid glycoprotein and the blood group A antigen, was shown to be present in RVs and RBCM-NPs, with CD47 also found to an almost equal degree on RBCs, RVs, and RBCM-NPs⁶⁶. The biological activity of membrane proteins expressed on the RBCM-NP surface can also be examined at the cellular level, especially the ability of CD47 to evade macrophage phagocytosis. Specifically, RBCM-NP uptake by mouse macrophage RAW264.7 cells was found to be 59.0% lower than that of naked nanoparticles⁵³. In addition, a saturation

in CD47 functionalization by the RBCM coating has been identified, below which approximately 92% of the input membrane proteins are used for particle functionalization, suggesting that the entire coating process is both reasonable and feasible⁵⁹. Determining the position and orientation of RBCM functional proteins after being coated on the nanoparticles is highly desirable. Membrane protein interactions with lipids were successfully investigated using cell blebs as an intermediate and determined using single molecule tracking and moment scaling spectrum analysis⁶⁷. Moreover, a geometry-based approach was developed by automatically inserting a membrane protein with a known 3D structure into membranes⁶⁸. These approaches may be consulted in revealing RBCM protein orientation.

5.3. Fluorescence colocalization

To further verify core-shell particle structure integrity, Hu et al.³⁸ designed a method wherein hydrophobic red DiD dyes and lipophilic green rhodamine-DMPE dyes were respectively loaded into the polymeric cores and RVs prior to their fusion. The resulting dual-fluorophore-labeled nanoparticles were incubated with HeLa cells for 6 h, after which DiD and rhodamine DMPE were observed to overlap at the same position using a fluorescence microscope. Fluorescence colocalization showed that the nanoparticles had a complete core-shell structure after being internalized by the cells, demonstrating the success of RBCM coating.

5.4. UV-vis absorption spectra

Encapsulation conditions can be also characterized by UV-vis absorption spectroscopy. Compared with the original nanoparticle absorption pattern, the encapsulated nanostructures retain the original absorption peak and obtain an extra absorption peak equivalent to the characteristic RV absorption peak^{50,69}. This result indicates a successful shift of the RVs on the nanoparticle surface without affecting the properties of the original nanoparticles.

Together, these *in vitro* characterizations verify the ideal state of RBC separation into vesicles and integration with nanoparticles.

6. RBCMs coated with different core nanoparticles for anti-tumor application

Subsequent research has allowed development of the coated core nanoparticles from the initial polymer nanoparticles to MNs, mesoporous silica nanoparticles (MSNs), upconversion nanoparticles (UCNPs), and gold nanoparticles (AuNPs) (Fig. 5).

6.1. Polymeric nanoparticles

6.1.1. Poly(*caprolactone*) (PCL) nanoparticles

PCL, with properties of biodegradability, biocompatibility, and low glass transition temperature, is used as a kind of polyester to construct core nanoparticles⁷⁰. Paclitaxel (PTX), a broad-spectrum antineoplastic agent, constitutes a commonly used model drug for treating various cancers including breast, ovarian, and lung cancers. Recently, RBCM-coated poly(*caprolactone*) nanoparticles loaded with PTX co-administered with a tumor penetrating peptide iRGD have been utilized for metastatic breast cancer treatment⁵³. The modified NPs showed significantly prolonged blood

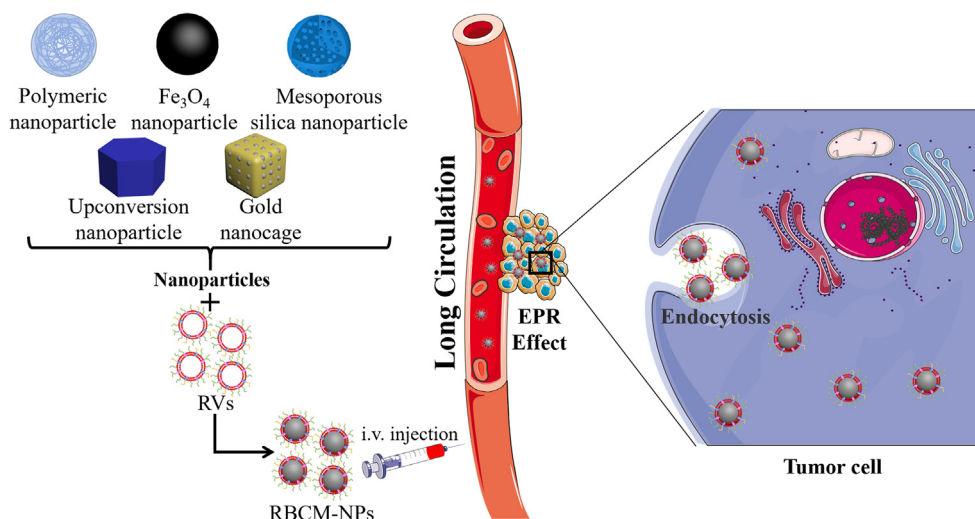


Figure 5 Red blood cell membrane-camouflaged nanoparticle achievement of antitumor effect. Different core nanoparticles are coated with RVs and then enter into the blood by intravenous (i.v.) injection, evading the immune system to realize long-term circulation, penetrate into the tumor tissues owing to the EPR effect, and finally enter into the tumor cells *via* endocytosis to achieve diagnosis and treatment of cancers.

circulation with a half elimination time 5.8-times that of the original polymer NPs. In addition, RBCM-mimetic nanoparticle co-administration with iRGD inhibited over 90% of tumor growth and suppressed 95% of lung metastases. The experimental data reveals the tremendous importance of long-term circulation and tumor penetration in the treatment of cancers, offering a new paradigm for nanocarrier design for delivering drugs to lung metastases-derived tumors.

However, lack of RBCM targeting ability for solid tumors is an obstacle to tumor cell internalization. Moreover, the diffusion barrier caused by complete RBCMs on the NP surface limits the effective release of loaded drugs^{71–73}. Therefore, some attempts have been implemented to solve these shortcomings, such as membrane surface modification to enhance its targeting and the combination of chemotherapy and phototherapy to promote the ablation of erythrocyte membranes, thereby promoting drug release. Su et al.⁷⁴ further designed novel near-infrared radiation (NIR) laser-responsive RBCM-NPs, in which the thermosensitive lipid DPPC is used in composite polymer cores. Under NIR laser stimulation, powerful thermal effects trigger DPPC phase change, destroying core structure and releasing PTX, which increased tumor cell uptake by 2.1-fold. The resulting antitumor effect representing marked optimization of previous RBCM-NPs and tumor penetration chemotherapy, suggesting that synergistic chemotherapy has advantages over single chemotherapy and may become an effective option for clinical treatment of metastatic breast cancer.

6.1.2. Polypyrrole (PPy) nanoparticles

PPy nanoparticles are considered as highly promising materials owing to their excellent photothermal and photoacoustic effects and are often used in PTT for tumors and as photoacoustic imaging (PAI) contrast agents for cancer diagnosis^{75–77}. Wang et al.⁶⁹ masked a layer of RBCMs on photothermal PPy nanoparticle surfaces; to further improve the photothermal effect, they used the endothelin A (ETA) receptor antagonist BQ123 to regulate the tumor microenvironment. BQ123 blocks ETA receptors, induces tumor vasodilatation, and increases blood perfusion by modulating the ET-1/ETA transduction pathway^{78,79}, which causes rapid of

tumor vessel diameter expansion by 20%–30%, thereby improving biomimetic PPy NP-directed targeted tumor delivery. The average tumor weight on day 13 was only 0.136 g, showing a better anti-tumor effect compared to other groups. The authors successfully achieved PAI and PTT under the dual action of RBCM-PPy NPs and ETA receptor antagonists, significantly increasing local PPy NP concentration in the tumor site.

6.1.3. Poly(lactide acid) (PLA) nanoparticles

PLA constitutes a promising material owing to its excellent biocompatibility, variable biodegradability, and commercial availability^{80–82}. Aryal et al.⁷⁴ used PLA nanoparticles as the core to compare the strategies of physically encapsulating and chemically conjugating doxorubicin (Dox) into RBCM-NPs as assessed *in vitro* using the myeloid leukemia cell line Kasumi-1 acute. When the Dox molecules were physically encapsulated in the polymer, 20% were released within the first 2 h, whereas only 5% were released following chemical conjugation. This suggests that chemical linkers responsive to the environment can achieve better controlled drug release^{83,84}. Moreover RBCM-NP release rate over about 72 h was about 20% whereas PEGylated NPs released 40% of Dox, demonstrating that RBCM cloaking provides a barrier that slows the outward diffusion of encapsulated drug molecules. These results indicate that nanoparticles covered by RBCMs represent a potential drug delivery platform for sustained release.

6.1.4. Poly(D,L-lactide-co-glycolide) (PLGA) nanoparticles

PLGA constitutes an FDA-approved polyester with adjustable biodegradability and good biocompatibility⁸⁵, which can be used to prepare nanoparticles by methods such as nanoprecipitation and emulsification^{72,86–88}. Hypoxia is a common pathological feature of most solid tumors⁸⁹. In cancer radiation therapy, oxygen can react with DNA and prevent DNA repair by tumor cells, thereby enhancing the killing effect⁹⁰. Perfluorocarbons (PFCs) are inert chemicals with extremely high oxygen solubility and can be used as an alternative to artificial blood^{91–93}. Gao et al.⁹⁴ obtained RBCM-PFC@PLGA-NPs by encapsulating PFCs in biocompatible PLGA and then coating with RBCMs. With efficient oxygen loading and drastically longer blood circulation times, RBCM-

PFC@PLGA-NPs could effectively deliver oxygen to the tumor after intravenous injection, thereby greatly relieving the tumor hypoxia and enhancing the therapeutic effect during radiotherapy. Zhang et al.⁹⁵ combined gambogic acid (GA)-loaded PLGA nanoparticles and RBCMs to assess the ability to preserve and enhance colorectal cancer treatment effects. RBCM-GA@PLGA-NPs were absorbed by gastrointestinal tract cells and inhibited SW480 cell proliferation *in vitro* via effects on apoptosis and cell cycle. *In vivo*, treated mice with free GA prolonged survival for 4 days compared to that of untreated mice, whereas treatment with RBCM-GA@PLGA-NPs extended survival for at least 30 days. Moreover, Luk et al.⁸ designed Dox-loaded PLGA nanoparticles coated with RBCMs for treating lymphomas and conducted a series of safety evaluations. This platform exhibited many necessary features for clinical DDS such as safety and biocompatibility, providing support for the continued development and clinical application of the RBCM-NP platform.

PH-sensitive polymeric nanoparticles (PGSC-PTX NPs) encapsulated with RBCMs have also been used in non-small cell lung cancer treatment strategies⁹⁶. Furthermore, the study of encapsulating polymer nanoparticles as nano-vaccines for the induction of antitumor immunity against melanoma⁹⁷ has also achieved remarkable results.

6.2. Fe_3O_4 nanoparticles

Fe_3O_4 core nanoparticles have proven to be useful for MRI, drug delivery, hyperthermia, and tissue repair owing to their unique magnetism, low toxicity, controlled size, good biodegradability, and biocompatibility, and have been intensively studied for diagnostic and therapeutic applications^{98–100}. To evade immune clearance and improve their systemic circulation time, Rao et al.¹⁰¹ designed an experimental program using RBCM-coated Fe_3O_4 NPs (RBCM- Fe_3O_4 -NPs). Compared with Fe_3O_4 and PEG- Fe_3O_4 -NPs, RBCM- Fe_3O_4 -NPs effectively reduced nanoparticle uptake by RAW 264.7 cells. In addition, RBCM- Fe_3O_4 -NPs and PEG- Fe_3O_4 -NPs respectively showed blood retentions of 14.2% and <6% ID/g after 24 h, further confirming that RBCM-NPs exhibit better blood retention than biopolymer-coated nanoparticles. With regard to biodistribution, RBCM- Fe_3O_4 -NP accumulation in the two major organs of the RES/MPS, the liver and spleen¹⁰², was 49.2 ± 7.1 and 100.1 ± 16.3 $\mu\text{g/g}$ respectively, whereas PEG- Fe_3O_4 -NP accumulation was 117.4 ± 30.3 and 174.5 ± 43.7 $\mu\text{g/g}$, demonstrating that RBCM coating can reduce RES/MPS absorption more effectively than PEGylation. Toward accelerating blood clearance, the second RBCM- Fe_3O_4 -NP injection had similar pharmacokinetic trends as the first; however, the second PEG- Fe_3O_4 -NP dose showed a dramatic decrease in the Fe content, suggesting a serious accelerated blood clearance (ABC) phenomenon in Fe_3O_4 @PEG nanoparticles, with anti-PEG antibody production likely responsible for the ABC phenomenon. Together, these data indicate that the RBCM coating can provide nanoparticles with a longer circulation time without causing ABC or inducing immune responses at the cellular (myeloid-derived suppressor cells) or humoral (IgM and IgG) level, thereby representing promising new technologies with tremendous clinical potential.

6.3. Magnetic nanoclusters (MNCs)

Highly crystallized iron oxide nanoparticles generated by pyrolysis have an exquisite polymer coating that shows a photothermal effect at higher concentrations^{103,104}. Ren et al.¹⁰⁵ in a comparative study on

individual Fe_3O_4 nanocrystals and Fe_3O_4 MNCs, found that MNCs have a better PTT effect than individual Fe_3O_4 nanoparticles. On this basis, they coated MNCs with RBCMs followed by intravenous injection in a xenograft mouse model of breast cancer assisted with PTT⁵⁰. In the cell uptake assay, 10^6 RAW264.7 cells absorbed 10.309 mg Fe in the MNC group, whereas only 4.417 mg Fe were taken up in the RBCM-MNC group, with 2.34-fold difference in cellular extrinsic Fe level. Owing to the diversity of membrane components, RBCM coatings can significantly reduce cell-level uptake of nonspecific nanoparticles. In the pharmacokinetic study, the MNCs were rapidly cleared from the bloodstream and could not be detected after 8 h, whereas the RBCM-MNCs exhibited a blood retention rate of approximately 10% ID/g 24 h after injection. In biodistribution, RBCM-MNC tumor uptake was $4.937 \pm 1.473\%$ and $2.630 \pm 0.602\%$ ID/g after 1 and 48 h following nanoparticle injection, whereas the MNC group showed only 1.282 ± 1.036 and $0.580 \pm 0.073\%$ ID/g. In addition, RBCM-MNC liver uptake at 1 and 48 h after injection was $17.743 \pm 5.547\%$ and $9.157 \pm 3.271\%$ ID/g, whereas that of MNC reached $32.110 \pm 5.812\%$ and $27.909 \pm 4.618\%$ ID/g, respectively. These data indicate that the RBCM coating strategy could significantly enhance tumor accumulation, reduce liver uptake, and achieve better biodistribution characteristics.

In the *in vivo* PTT antitumor effect study of RBCM-MNCs, the authors set up saline, MNC, RBCM-MNC, and RBCM-MNC with the magnetic field groups, and were illuminated with the same laser setting. Thermal images of mice from the different treatment groups showed that the temperature of both RBCM-MNC groups rose rapidly above 50 °C compared to that of the other two groups, which indicated that RBCM-MNCs could efficiently convert light into heat, and showed a higher photothermal effect than the original MNCs, demonstrating that the camouflage coating allowed for increased tumor accumulation and preferred biodistribution. Finally, the MNC, RBCM-MNC, and RBCM-MNC with magnetic field group tumor inhibition rates calculated by tumor weight were 21.43%, 93.81%, and 94.24%, respectively. RBC-derived membranes afford significantly increased MNC blood retention and invisibility, providing RBCM-MNCs with strong passive EPR effects even in magnetic-field free condition. These suggest the potential of iron-based nanomaterials for imaging and therapeutic applications and provide guidelines for combining nano-bionics with other physical techniques such as PTT and photodynamic therapy (PDT)¹⁰⁶ to treat cancer.

6.4. Mesoporous silica nanoparticles (MSNs)

MSNs have been widely used for anticancer drug delivery¹⁰⁷ because of their large surface area and adjustable pore size. However, MSNs are prone to aggregation, leakage, and limited circulation time in the blood, which limit their anti-cancer efficacy. Su et al.¹⁰⁸ achieved high loading capacity by masking MSNs with RBCMs to load the anticancer drug Dox and the near-infrared photosensitizer chlorin e6 (Ce6). Lipid-coated MSN (L-MSNs) were also used. Lipid coating did not reduce MSN cellular uptake, confirming the superiority of RBCM protein in reducing macrophage uptake. *In vitro* laser-induced RBCM-MSN-Dox/Ce6 respectively induced 1.9-, 2.0-, and 2.0-fold Dox accumulation after 1, 2, and 4 h of incubation compared to that without laser. This was suggested to arise from reactive oxygen species (ROS) produced by Ce6 laser stimulation, which oxidize and form defective phospholipid molecules in RBCMs and cancer cell

membranes, affecting cell membrane permeabilization, resulting in increased cellular uptake of released Dox¹⁰⁹. In terms of cytotoxicity, RBCM-MSN-Dox and RBCM-MSN-Dox/Ce6+Laser IC₅₀ values on 4T1 cells were 2.6 and 0.9 µg/mL, which was 1.4- and 1.5-fold lower than that of MSN-Dox (3.7 µg/mL) and MSN-Dox/Ce6+Laser (1.6 µg/mL), potentially because RBCM coating can prevent MSN drug leakage and premature release. In addition, the RBCM-MSN-Dox/Ce6 tumor inhibition rate was 91.4%, significantly higher than that of RBCM-Ce6+Laser (68.9%) and RBCM-Dox (73.7%). These results indicate that RBCM-MSN-Dox/Ce6, when combined with laser light stimulation, can combine the synergistic effects of chemotherapy and PDT to achieve the most efficient cytotoxicity. Moreover, as demonstrated by hematoxylin and eosin (H&E) staining, laser-induced RBCM-MSN-Dox/Ce6 obviously enhanced anti-metastatic function, with no metastases being found in the lungs.

6.5. Upconversion nanoparticles (UCNPs)

UCNPs have excellent chemical and optical properties, low toxicity, and good light stability compared to traditional down-conversion fluorescent nano-probes^{110–116}. Ding et al.¹⁰⁶ have developed a new type of bionic PDT nanocarrier (F/P-RM-U_s/PS) using UCNPs with incorporated photosensitizers (PS) as the cores, coated by the RBCMs modified with folic acid (FA) and triphenylphosphonium (TPP) to achieve dual targeting of cancer cells and mitochondria. Compared with other conventional coatings, RBCM coating significantly promoted ground state molecular oxygen (³O₂) entry into the agent core for ¹O₂ production. Specifically, the F/P-RM-U_s/PS group exhibited over 4-fold higher intracellular ¹O₂ concentration than the U_s/PS group. At 20 days after PDT treatment using F/P-RM-U_s/PS, tumor volume was only one tenth that using U_s/PS. The design of PDT agents yielded a programmed boost in blood circulation, tumor accumulation, cellular uptake, mitochondria guidance, and ¹O₂ transportation, providing the first example of RBCM-masked PDT nanocarriers with programmed delivery.

6.6. Gold nanoparticles (AuNPs)

Owing to their biocompatibility, optical properties, and easily modifiable surfaces, AuNPs are often used as imaging agents and drug carriers^{117,118}. Gold nanocages (AuNCs) and gold nanoshells have been studied because hollow nanoparticles are more efficient at converting light to heat^{71,119–121}. In studies by Piao et al.⁷¹, RBCM coatings significantly prolonged AuNC half-life in the circulation, leading to two-fold in-tumor deposition at 24 and 48 h after injection compared with PVP-modified AuNCs. Moreover, tumor-bearing mice treated with RBCM-AuNCs achieved 100% survival over 45 days.

6.7. Gelatin nanoparticles

It is well-known that broad-spectrum bacteria secrete gelatinases, which can effectively hydrolyze gelatin nanoparticles to small biomolecules¹²². Therefore, Li et al.¹²³ proposed an antibiotic delivery system based on supramolecular gelatin nanoparticles (SGNPs) that activates its release mechanisms in the presence of gelatinase. The SGNPs were first decorated with vancomycin (Van), a model antibiotic, and then coated with RBCMs to obtain the novative and biomimetic antibiotic delivery system

(Van ⊂ SGNPs@ RBC). Studies have shown that this delivery system effectively and specifically released antibiotics at the site of infection. By coating the RBCMs, Van ⊂ SGNPs@ RBC showed excellent immune evasion and alleviated symptoms caused by bacterial infection. It is believed that with the use of different antibiotics and bioresponsive materials, the system can achieve efficient and specific killing of various bacteria.

Notably, each type of core nanoparticles has its own advantages (Table 1). The choice of nanoparticle species plays an important role in the size and shape of the formulation as well as subsequent drug release. Different designs should therefore be developed according to the specific situation.

7. Surface modification of erythrocyte membranes

In the application of RBCM-NPs for the treatment of diseases, especially for cancers, it is desirable to overcome the obstacles in the process of tumor cell internalization. This is typically achieved by surface modification to increase the ability of the liquid to penetrate the tissue or by carrier functionalization with a ligand that targets the overexpressed tumor antigen to enable cancer targeting and minimize side effects¹²⁴. Zhou et al.⁶⁴ stably anchored recombinant hyaluronidase, PH20 (rHuPH20) molecules on the RBCM outer domain by using a cell-impermeable linker, NHS-PEG-maleimide, while retaining their enzymatic activity. The functionalized RBCMs were then used to coat nanoparticles. The RBCM-NPs alone diffused little into extracellular matrix (ECM)-mimicking gels whereas rHuPH20-conjugated RBCM-NPs in the gel doubled the free rHuPH20 diffusion efficiency, with the same enzymatic activity. In PC3 cells, the conjugated rHuPH20 increased the amount internalized or bound to PC3 cells three-fold compared to that of RBC-NP with 10 U free rHuPH20. These results suggested that the conjugated rHuPH20 could more effectively assist NP diffusion in ECM-mimicking gels as well as in the cytoplasmic HA matrix of PC3 cells. Moreover, rHuPH20 modification did not reduce the RBCM-NP blood circulation time. This surface modification method thus preserves the inherent native cell membrane characteristics while adding other required functions.

Targeting selection is a necessary tool in the use of RBCM-NPs for the treatment of cancers, which can effectively avoid side effects of drugs on normal cells and tissues^{125–128}. At present, there are many ongoing attempts to improve its targeting efficacy, which include chemical conjugation of carboxyl-, amine-, or sulfhydryl- groups on the surface of cell membranes^{129–135}. However, these methods will lead to chemical reactions and inactivation of membrane proteins on the surface of RBCM membranes, consequently destroying its original immune escape function. Thus, Fang et al.¹³⁶ proposed a lipid insertion method for functionalizing RBCMs membranes, using ligand-linker-lipid conjugates as targeting ligands. In this study, folate with small molecular and nucleolin-targeting aptamer AS1411 with larger molecules was used as ligands to form targeting ligands. By flow cytometric and fluorescence imaging analysis, it was found that the model cancer cells' uptake of modified erythrocyte membrane-coated nanoparticles were respectively 8- and 2-fold as compared to unmodified cells, showing a pronounced targeting effect¹³⁶. Through the aid of lipid chains and the dynamic membrane bilayer structure, the targeting ligand can spontaneously enter the surface of the cell membrane, effectively avoiding the exposure of the membrane proteins to chemical reactions. The complete release of the drug becomes a critical issue after the increasing the uptake of

Table 1 Studies on different inner cores of RBCM-NPs for cancer therapy.

| Inner core | Advantage | Application | Ref. |
|---|--|--|----------|
| Polymeric nanoparticles | Biodegradability; Biocompatibility; Low glass transition temperature | Loaded with PTX co-administered with iRGD/combined with PTT for the treatment of metastatic breast cancer | 53,70,74 |
| PPy nanoparticles | Biocompatibility; Low cytotoxicity; Excellent photothermal and photoacoustic effects | Under dual action of biomimetic and ETA receptor antagonists to achieve PAI and PTT | 69 |
| PLA nanoparticles | Biocompatibility; Biodegradability | Loaded with Dox for studies of controlled drug loading and release | 73 |
| PLGA nanoparticles | Biocompatibility; Biodegradability; Sustained drug release | Loaded with PFC to relieve tumor hypoxia; Loaded with GA for the treatment of colorectal cancer | 8,94,95 |
| Fe ₃ O ₄ nanoparticles (Fe ₃ O ₄ NPs) | Unique magnetism; Low toxicity; Controlled size | For evading immune clearance and improving circulation time | 101 |
| Magnetic nanoparticles (MNs) | Better PTT effect | Curing breast cancer xenograft mice in conjunction with PTT | 50 |
| Mesoporous silica nanoparticles (MSNs) | Large surface area; Adjustable pore size | Loaded with Dox and Ce6 combined with <i>in vitro</i> laser triggering to treat metastatic breast cancer | 108 |
| Upconversion nanoparticles (UCNPs) | Low toxicity; Good photo-stability; Superior chemical and optical properties | Incorporated UCNPs with PS, and RBCMs modified with DSPE-PEG2000-FA and DSPE-PEG2000-TPP to develop a new type of bionic PDT nanocarrier | 106 |
| Gold nanoparticles (AuNPs) | Biocompatibility; Good optical properties; Easily modifiable surface | AuNCs coated with RBCMs to prolong half-life | 71 |
| Gelatin nanoparticles | Can be hydrolyzed into small biomolecules by gelatinases secreted by bacteria | For reducing clearance by the immune system and absorbing the bacterial exotoxin to relieve bacterial infection | 123 |

the carrier by the tumor cells through targeting modification. It can be used in the form of phototherapy combined with chemotherapy, using light-sensitive nanocarriers^{60,69,71,105} or co-loaded chemotherapeutic agents and PS to increase drug release, achieving excellent anti-tumor effects (Fig. 6).

In general, UCNPs are ligand-modified for targeting of cancers; however, nanoparticles in biological fluids would form “protein corona” that cover the ligands on the surface of the nanoparticles and reduce their targeting features. Recently, Rao et al.¹³⁷ reported that modification of FA with UCNPs coated with erythrocyte membranes effectively prevented protein adsorption, thereby enhancing targeting efficiency and *in vivo* tumor imaging. Besides, a brain-targeted delivery system that combines RBCM-NPs with unique neurotoxin-derived targeting moieties, “CDX peptides” has been shown to have potent brain targeting abilities, and to significantly reduce drug toxicity¹³⁸. The highlight of this study is its effective combination of natural immune escape and cancer-targeted therapy, that are both pivotal in the treatment of cancers, and the next step may be to study the effect of targeting ligands on RBCM-NPs *in vivo* and to further demonstrate the promising cancer treatment prospects of this technique.

Apart from the membrane surface modifications (Table 2), the concept of membranes fusion to produce new bio-coatings by fusing two different sources of cell membranes has been proposed¹⁷. They coated the PLGA cores with the hybrid membrane fused by erythrocyte membrane and the platelet membrane that has been extensively used for nano-coating to enhance targeting in recent years. After a series of *in vitro* and *in vivo* characterizations, the authors confirmed the successful transfer of the protein markers on the membrane surface and further demonstrated that RBC-platelet hybridization membrane allows the PLGA cores to function simultaneously with immune escape and targeting¹⁷. This provides a strong guide to retain the natures of different cells by the fusion of other specific functional membranes, thereby overcoming the limitations of the current multi-functional modifications of nanoparticles. In addition, the technology can improve the applicability of emerging nano-carriers with complex surface chemistry, and opens up a new field for the further developments of biomimetic nanoparticles.

8. Conclusions

It is a daunting task to artificially replicate the biological interactions that occurs in the body. Researchers are more inclined to seek inspiration from nature instead of creating new solutions from scratch. Using erythrocyte membranes as drug carriers for novel DDS has become an interesting strategy for the functionalization of nanomaterials and will remain an active area in future researches. We can draw blood from the patient, coat the various nanoparticle cores with derivatized RBC vesicles and then inject them back into the same patient for treatment or diagnosis. Erythrocyte membrane-coated nanoparticles have achieved a transition from the “stealth” of original prevalent PEGylation to the “disguise” of erythrocyte membrane-coating, achieving the same surface conditions with the RBCs in the blood, thus escaping phagocytosis by the immune system. Coating of nanostructures with vesicles derived from native cell membranes imparts the intrinsic functions and characteristics of the source cells to the nanostructures due to the transport of many membrane proteins, glycans, and lipids to the surface of the original nanoparticles. These cell-membrane-coated nanoparticles can retain their cell-surface coating properties in interaction with other cells and pathogenic agents and

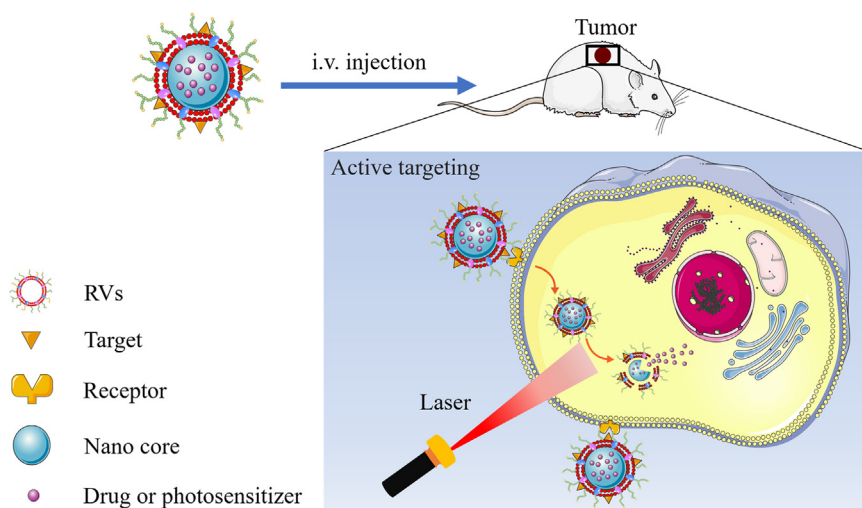


Figure 6 Schematic design of ligand-modified drug or photosensitizer-loaded RBCM-NPs combined with phototherapy for targeting and sequential drug delivery. Ligand-modified RBCM-NPs are injected into mice to achieve active targeting into tumor cells. Under laser irradiation, light-sensitive nanocarriers or PS can provide strong thermal energy, triggering the destruction of cores and resulting in the release of PTX.

Table 2 Currently surface modifications of RBCMs for antitumor application.

| Modified ligand | Function | Ref. |
|---|--|-------------|
| Folic acid (FA) | Selective recognition of cancer cells; effectively preventing “protein adsorption” on the surface of nanoparticles | 106,136,137 |
| Triphenylphosphonium (TPP) | Targeting to mitochondria and enhancing the yield of $^1\text{O}_2$ | 106 |
| rHuPH20 | Assisting nanoparticle diffusion in the cytoplasmic HA matrix of PC3 cells | 64 |
| Aptamer AS1411 | Showing targeting capability against several cancer cell types | 136 |
| CDx peptides | Ability to traverse the blood–brain barrier and achieve marked therapeutic efficacy in glioma treatment | 138 |
| Mannose | Actively targeting APCs (antigen presenting cells) in lymphatic organs | 97 |
| Anti-EpCam (epithelial cell adhesion molecule) antibodies | Exhibiting better targeting capacity of 4T1 cells compared to unmodified nanoparticles | 139 |
| RGD (Arg–Gly–Asp) | Realizing stronger tumor growth inhibition effects than typical tumor-targeting peptides | 140 |

achieve a wide variety of therapeutic purposes. In addition to the direct anti-tumor effect of the coated nano-preparation, there are already cases in which the polymeric nanoparticles encapsulated by the erythrocyte membranes as a nano vaccine to achieve anti-tumor immunity. At the same time, as it comes from homologous erythrocytes, it can bypass the complex processes of protein identification, purification, and conjugation. Prior studies focused on the development and applications of RBCMs coated with spherical metal oxide particles or PLGA nanoparticles. In future, we may be able to overcome this limitation and extend this coating technology to other types and shapes of nanostructures. At the same time, various external stimuli such as near infrared-mediated photothermal effects, ultrasound¹⁴¹ and magnetocaloric therapies have now been tried to enable the drug to be released on demand, which will be a new and broader area to study.

The effective transportation and long-circulating half-life of erythrocytes demonstrate their unique advantages in anti-tumor drug delivery and have also stimulated scientists to develop and utilize other source cell membranes for nano-coating, based on the characteristics of the corresponding diseases. Various membranes including platelet membranes, neutrophil membranes, tumor cell membranes, and bacterial membranes have been used in many fields, such as anti-tumor, detoxification, and immunomodulation,

and have achieved considerably good experimental results. In the successful case of the fusion of erythrocyte membrane and platelet membrane coated nanoparticles, we can also select two or more cell membranes with the corresponding functionalities for fusion experiments according to the needs of the treatment of the diseases, but their characterizations and verifications can be relatively complicated and require precise and elegant designs. With the assistance of nanotechnology and molecular biology, it is believed that researchers can design better synthetic delivery vehicles for more efficient loading.

At present, the technology for preparing nanoparticles and erythrocyte membrane-derived vesicles is relatively mature, and they can be produced independently without interfering with each other and have relatively high flexibility. Therefore, it is completely possible to realize large-scale production. However, the biggest challenge is getting acceptable batch-to-batch variation, and the fusion process must be scalable and optimized to maximize efficiency. Quality control of RBCM-NPs is another major challenge that must be addressed. It must be ensured that erythrocyte membranes are not contaminated by pyrogens and viruses, and that RBCM-NPs with denatured proteins should be eliminated to prevent potential immune responses to endogenous

antigens^{51,142}. Meanwhile, it should be emphasized that since the systems are composed of biological materials, there are complex regulatory issues while using them for clinical applications. Despite various challenges that may come up in the future, this biomimetic nanosystem that combines natural and synthetic biomaterials provides a unique and exciting strategy for targeting tumor, and it is also a new paradigm of thinking.

References

- Kang L, Gao Z, Huang W, Jin M, Wang Q. Nanocarrier-mediated co-delivery of chemotherapeutic drugs and gene agents for cancer treatment. *Acta Pharm Sin B* 2015;**5**:169–75.
- Weng Y, Liu J, Jin S, Guo W, Liang X, Hu Z. Nanotechnology-based strategies for treatment of ocular disease. *Acta Pharm Sin B* 2017;**7**:281–91.
- Fang J, Qin H, Nakamura H, Tsukigawa K, Shin T, Maeda H. Carbon monoxide, generated by heme oxygenase-1, mediates the enhanced permeability and retention effect in solid tumors. *Cancer Sci* 2012;**103**:535–41.
- Iwamoto T. Clinical application of drug delivery systems in cancer chemotherapy: review of the efficacy and side effects of approved drugs. *Biol Pharm Bull* 2013;**36**:715–8.
- Chen MC, Lin ZW, Ling MH. Near-infrared light-activatable microneedle system for treating superficial tumors by combination of chemotherapy and photothermal therapy. *ACS Nano* 2016;**10**:93–101.
- Veronese FM, Pasut G. PEGylation, successful approach to drug delivery. *Drug Discov Today* 2005;**10**:1451–8.
- Harris JM, Chess RB. Effect of pegylation on pharmaceuticals. *Nat Rev Drug Discov* 2003;**2**:214–21.
- Luk BT, Fang RH, Hu CM, Copp JA, Thamphiwatana S, Dehaini D, et al. Safe and immunocompatible nanocarriers cloaked in RBC membranes for drug delivery to treat solid tumors. *Theranostics* 2016;**6**:1004–11.
- Rao L, Bu LL, Cai B, Xu JH, Li A, Zhang WF, et al. Cancer cell membrane-coated upconversion nanoprobe for highly specific tumor imaging. *Adv Mater* 2016;**28**:3460–6.
- Jin K, Luo Z, Zhang B, Pang Z. Biomimetic nanoparticles for inflammation targeting. *Acta Pharm Sin B* 2018;**8**:23–33.
- Ha D, Yang N, Nadithe V. Exosomes as therapeutic drug carriers and delivery vehicles across biological membranes: current perspectives and future challenges. *Acta Pharm Sin B* 2016;**6**:287–96.
- Huang Y, Gao X, Chen J. Leukocyte-derived biomimetic nanoparticulate drug delivery systems for cancer therapy. *Acta Pharm Sin B* 2018;**8**:4–13.
- Ihler GM, Glew RH, Schnure FW. Enzyme loading of erythrocytes. *Proc Natl Acad Sci U S A* 1973;**70**:2663–6.
- Piergè F, Serafini S, Rossi L, Magnani M. Cell-based drug delivery. *Adv Drug Deliv Rev* 2008;**60**:286–95.
- Hamidi M, Tajerzadeh H. Carrier erythrocytes: an overview. *Drug Deliv* 2003;**10**:9–20.
- Patel PD, Dand N, Hirlekar RS, Kadam VJ. Drug loaded erythrocytes: as novel drug delivery system. *Curr Pharm Des* 2008;**14**:63–70.
- Dehaini D, Wei X, Fang RH, Masson S, Angsantikul P, Luk BT, et al. Erythrocyte-platelet hybrid membrane coating for enhanced nanoparticle functionalization. *Adv Mater* 2017;**29**:1606209.
- Yoo JW, Irvine DJ, Discher DE, Mitragotri S. Bio-inspired, bioengineered and biomimetic drug delivery carriers. *Nat Rev Drug Discov* 2011;**10**:521–35.
- Wang C, Sun X, Cheng L, Yin S, Yang G, Li Y, et al. Multifunctional theranostic red blood cells for magnetic-field-enhanced *in vivo* combination therapy of cancer. *Adv Mater* 2014;**26**:4794–802.
- Sun X, Wang C, Gao M, Hu A, Liu Z. Remotely controlled red blood cell carriers for cancer targeting and near-infrared light-triggered drug release in combined photothermal-chemotherapy. *Adv Funct Mater* 2016;**12**:548.
- Doshi N, Zahr AS, Bhaskar S, Lahann J, Mitragotri S. Red blood cell-mimicking synthetic biomaterial particles. *Proc Natl Acad Sci U S A* 2009;**106**:21495–9.
- Tsai RK, Rodriguez PL, Discher DE. Self inhibition of phagocytosis: the affinity of 'marker of self' CD47 for SIRP alpha dictates potency of inhibition but only at low expression levels. *Blood Cells Mol Dis* 2010;**45**:67–74.
- Merkel TJ, Jones SW, Herlihy KP, Kersey FR, Shields AR, Napier M, et al. Using mechanobiological mimicry of red blood cells to extend circulation times of hydrogel microparticles. *Proc Natl Acad Sci U S A* 2011;**108**:586–91.
- Marsden NV, Ostling SG. Accumulation of dextran in human red cells after haemolysis. *Nature* 1959;**184**(Suppl 10):723–4.
- Jain S, Jain NK. Engineered erythrocytes as a drug delivery system. *Indian J Pharm Sci* 1997;**59**:275–81.
- Hu CM, Fang RH, Zhang L. Erythrocyte-inspired delivery systems. *Adv Healthc Mater* 2012;**1**:537–47.
- Lejeune A, Moorjani M, Gicquaud C, Lacroix J, Poyet P, Gaudreault R. Nanoerythrocyte, a new derivative of erythrocyte ghost: preparation and antineoplastic potential as drug carrier for daunorubicin. *Anticancer Res* 1994;**14**:915–9.
- Desilets J, Lejeune A, Mercer J, Gicquaud C. Nanoerythrocytes, a new derivative of erythrocyte ghost: iv. Fate of reinjected nanoerythrocytes. *Anticancer Res* 2001;**21**:1741–7.
- Hu CM, Fang RH, Copp J, Luk BT, Zhang L. A biomimetic nanosponge that absorbs pore-forming toxins. *Nat Nanotechnol* 2013;**8**:336–40.
- Brown E. Integrin-associated protein (CD47): an unusual activator of G protein signaling. *J Clin Invest* 2001;**107**:1499–500.
- Oldenburg PA, Zheleznyak A, Fang YF, Lagenaur CF, Gresham HD, Lindberg FP. Role of CD47 as a marker of self on red blood cells. *Science* 2000;**288**:2051–4.
- Barclay AN, Van den Berg TK. The interaction between signal regulatory protein alpha (SIRPalpha) and CD47: structure, function, and therapeutic target. *Annu Rev Immunol* 2014;**32**:25–50.
- Kroll AV, Fang RH, Zhang L. Biointerfacing and applications of cell membrane-coated nanoparticles. *Bioconjug Chem* 2017;**28**:23–32.
- Schonermark S, Rauterberg EW, Shin ML, Loke S, Roelcke D, Hansch GM. Homologous species restriction in lysis of human erythrocytes: a membrane-derived protein with C8-binding capacity functions as an inhibitor. *J Immunol* 1986;**136**:1772–6.
- Zalman LS, Wood LM, Muller-Eberhard HJ. Isolation of a human erythrocyte membrane protein capable of inhibiting expression of homologous complement transmembrane channels. *Proc Natl Acad Sci U S A* 1986;**83**:6975–9.
- Kim DD, Miwa T, Kimura Y, Schwendener RA, Van LCM, Song WC. Deficiency of decay-accelerating factor and complement receptor 1-related gene/protein y on murine platelets leads to complement-dependent clearance by the macrophage phagocytic receptor CR1g. *Blood* 2008;**112**:1109–19.
- Fang RH, Hu CM, Zhang L. Nanoparticles disguised as red blood cells to evade the immune system. *Expert Opin Biol Ther* 2012;**12**:385–9.
- Hu CM, Zhang L, Aryal S, Cheung C, Fang RH, Zhang L. Erythrocyte membrane-camouflaged polymeric nanoparticles as a biomimetic delivery platform. *Proc Natl Acad Sci U S A* 2011;**108**:10980–5.
- Ihler GM, Tsang HC. Hypotonic hemolysis methods for entrapment of agents in resealed erythrocytes. *Methods Enzymol* 1987;**149**:221–9.
- Sato Y, Yamakose H, Suzuki Y. Mechanism of hypotonic hemolysis of human erythrocytes. *Biol Pharm Bull* 1993;**16**:506–12.
- Seth M, Ramachandran A, Leal LG. Dilution technique to determine the hydrodynamic volume fraction of a vesicle suspension. *Langmuir* 2010;**26**:15169–76.
- Bird J, Best R, Lewis DA. The encapsulation of insulin in erythrocytes. *J Pharm Pharmacol* 1983;**35**:246–7.
- Gutierrez MC, Zarzuelo CA, Sayalero MM, Lanao JM. Factors associated with the performance of carrier erythrocytes obtained by hypotonic dialysis. *Blood Cells Mol Dis* 2004;**33**:132–40.

44. Tajerzadeh H, Hamidi M. Evaluation of hypotonic preswelling method for encapsulation of enalaprilat in intact human erythrocytes. *Drug Dev Ind Pharm* 2000;**26**:1247–57.
45. Hamidi M, Zarrin AH, Foroozesh M, Zarei N, Mohammadi-Samani S. Preparation and *in vitro* evaluation of carrier erythrocytes for RES-targeted delivery of interferon- α 2b. *Int J Pharm* 2007;**341**:125–33.
46. Franco RS, Barker R, Novick S, Weiner M, Martelo OJ. Effect of inositol hexaphosphate on the transient behavior of red cells following a DMSO-induced osmotic pulse. *J Cell Physiol* 1986;**129**:221–9.
47. Watts TJ, Handy RD. The haemolytic effect of verapamil on erythrocytes exposed to varying osmolarity. *Toxicol Vitro* 2007;**21**:835–9.
48. Lynch AL, Chen R, Slater NK. pH-responsive polymers for trehalose loading and desiccation protection of human red blood cells. *Biomaterials* 2011;**32**:4443–9.
49. Choi SO, Kim YC, Park JH, Hutcheson J, Gill HS, Yoon YK, et al. An electrically active microneedle array for electroporation. *Biomed Microdevices* 2010;**12**:263–73.
50. Ren X, Zheng R, Fang X, Wang X, Zhang X, Yang W, et al. Red blood cell membrane camouflaged magnetic nanoclusters for imaging-guided photothermal therapy. *Biomaterials* 2016;**92**:13–24.
51. Zhai Y, Su J, Ran W, Zhang P, Yin Q, Zhang Z, et al. Preparation and application of cell membrane-camouflaged nanoparticles for cancer therapy. *Theranostics* 2017;**7**:2575–92.
52. Hu CM, Fang RH, Wang KC, Luk BT, Thamphiwatana S, Dehaini D, et al. Nanoparticle biointerfacing by platelet membrane cloaking. *Nature* 2015;**526**:118–21.
53. Su J, Sun H, Meng Q, Yin Q, Tang S, Zhang P, et al. Long circulation red-blood-cell-mimetic nanoparticles with peptide-enhanced tumor penetration for simultaneously inhibiting growth and lung metastasis of breast cancer. *Adv Funct Mater* 2016;**26**:1243–52.
54. Schauer R. Sialic acids as regulators of molecular and cellular interactions. *Curr Opin Struct Biol* 2009;**19**:507–14.
55. Kelm S, Schauer R. Sialic acids in molecular and cellular interactions. *Int Rev Cytol* 1997;**175**:137–240.
56. Raveendran P, Fu J, Wallen SL. Completely “green” synthesis and stabilization of metal nanoparticles. *J Am Chem Soc* 2003;**125**:13940–1.
57. Lemarchand C, Gref R, Couvreur P. Polysaccharide-decorated nanoparticles. *Eur J Pharm Biopharm* 2004;**58**:327–41.
58. Luk BT, Hu CM, Fang RH, Dehaini D, Carpenter C, Gao W, et al. Interfacial interactions between natural RBC membranes and synthetic polymeric nanoparticles. *Nanoscale* 2014;**6**:2730–7.
59. Hu CM, Fang RH, Luk BT, Chen KN, Carpenter C, Gao W, et al. “Marker-of-self” functionalization of nanoscale particles through a top-down cellular membrane coating approach. *Nanoscale* 2013;**5**:2664–8.
60. Rao L, Cai B, Bu LL, Liao QQ, Guo SS, Zhao XZ, et al. Microfluidic electroporation-facilitated synthesis of erythrocyte membrane-coated magnetic nanoparticles for enhanced imaging-guided cancer therapy. *ACS Nano* 2017;**11**:3496–505.
61. Miyazaki J, Aihara H. Gene transfer into muscle by electroporation *in vivo*. *Methods Mol Med* 2002;**69**:49–62.
62. Zhang J, Gao W, Fang RH, Dong A, Zhang L. Synthesis of nanogels via cell membrane-templated polymerization. *Small* 2015;**11**:4309–13.
63. Hochmuth RM, Evans CA, Wiles HC, McCown JT. Mechanical measurement of red cell membrane thickness. *Science* 1983;**220**:101–2.
64. Zhou H, Fan Z, Lemons PK, Cheng H. A facile approach to functionalize cell membrane-coated nanoparticles. *Theranostics* 2016;**6**:1012–22.
65. Gagneux P, Varki A. Evolutionary considerations in relating oligosaccharide diversity to biological function. *Glycobiology* 1999;**9**:747–55.
66. Rodriguez PL, Harada T, Christian DA, Pantano DA, Tsai RK, Discher DE. Minimal “Self” peptides that inhibit phagocytic clearance and enhance delivery of nanoparticles. *Science* 2013;**339**:971–5.
67. Richards MJ, Hsia CY, Singh RR, Haider H, Kumpf J, Kawate T, et al. Membrane protein mobility and orientation preserved in supported bilayers created directly from cell plasma membrane blebs. *Langmuir* 2016;**32**:2963–74.
68. Kimmett T, Smith N, Witham S, Petukh M, Sarkar S, Alexov E. ProBLM web server: protein and membrane placement and orientation package. *Comput Math Methods Med* 2014;**2014**:838259.
69. Wang X, Li H, Liu X, Tian Y, Guo H, Jiang T, et al. Enhanced photothermal therapy of biomimetic polypyrrole nanoparticles through improving blood flow perfusion. *Biomaterials* 2017;**143**:130–41.
70. Sinha VR, Bansal K, Kaushik R, Kumria R, Trehan A. Poly-epsilon-caprolactone microspheres and nanospheres: an overview. *Int J Pharm* 2004;**278**:1–23.
71. Piao JG, Wang L, Gao F, You YZ, Xiong Y, Yang L. Erythrocyte membrane is an alternative coating to polyethylene glycol for prolonging the circulation lifetime of gold nanocages for photothermal therapy. *ACS Nano* 2014;**8**:10414–25.
72. Fang RH, Hu CM, Luk BT, Gao W, Copp JA, Tai Y, et al. Cancer cell membrane-coated nanoparticles for anticancer vaccination and drug delivery. *Nano Lett* 2014;**14**:2181–8.
73. Aryal S, Hu CM, Fang RH, Dehaini D, Carpenter C, Zhang DE, et al. Erythrocyte membrane-cloaked polymeric nanoparticles for controlled drug loading and release. *Nanomed (Lond)* 2013;**8**:1271–80.
74. Su J, Sun H, Meng Q, Yin Q, Zhang P, Zhang Z, et al. Bioinspired nanoparticles with NIR-controlled drug release for synergetic chemophotothermal therapy of metastatic breast cancer. *Adv Funct Mater* 2016;**26**:7495–506.
75. Zha Z, Deng Z, Li Y, Li C, Wang J, Wang S, et al. Biocompatible polypyrrole nanoparticles as a novel organic photoacoustic contrast agent for deep tissue imaging. *Nanoscale* 2013;**5**:4462–7.
76. Jin Y, Li Y, Ma X, Zha Z, Shi L, Tian J, et al. Encapsulating tantalum oxide into polypyrrole nanoparticles for X-ray CT/photoacoustic bimodal imaging-guided photothermal ablation of cancer. *Biomaterials* 2014;**35**:5795–804.
77. Li J, Arnal B, Wei CW, Shang J, Nguyen TM, O'Donnell M, et al. Magneto-optical nanoparticles for cyclic magnetomotive photoacoustic imaging. *ACS Nano* 2015;**9**:1964–76.
78. Martinive P, De Wever J, Bouzin C, Baudelet C, Sonveaux P, Gregoire V, et al. Reversal of temporal and spatial heterogeneities in tumor perfusion identifies the tumor vascular tone as a tunable variable to improve drug delivery. *Mol Cancer Ther* 2006;**5**:1620–7.
79. Sonveaux P, Dessy C, Martinive P, Havaux X, Jordan BF, Gallez B, et al. Endothelin-1 is a critical mediator of myogenic tone in tumor arterioles: implications for cancer treatment. *Cancer Res* 2004;**64**:3209–14.
80. Shive MS, Anderson JM. Biodegradation and biocompatibility of PLA and PLGA microspheres. *Adv Drug Deliv Rev* 2012;**64**:5–24.
81. Hamid ZAA, Tham CY, Ahmad Z. Preparation and optimization of surface-engineered poly(lactic acid) microspheres as a drug delivery device. *J Mater Sci* 2018;**53**:4745–58.
82. Tawakkal IS, Cran MJ, Miltz J, Bigger SW. A review of poly(lactic acid)-based materials for antimicrobial packaging. *J Food Sci* 2014;**79**:1477–90.
83. Aryal S, Hu CM, Zhang L. Polymer-cisplatin conjugate nanoparticles for acid-responsive drug delivery. *ACS Nano* 2010;**4**:251–8.
84. Gao W, Chan JM, Farokhzad OC. pH-Responsive nanoparticles for drug delivery. *Mol Pharm* 2010;**7**:1913–20.
85. McCall RL, Sirianni RW. PLGA nanoparticles formed by single- or double-emulsion with vitamin E-TPGS. *J Vis Exp* 2013:51015.
86. Alshamsan A. Nanoprecipitation is more efficient than emulsion solvent evaporation method to encapsulate curcubitacin I in PLGA nanoparticles. *Saudi Pharm J* 2014;**22**:219–22.
87. Lin HJ, Wang JH, Wang CY, Wu YC. The preparation and characteristic of poly(lactide-co-glycolide) microspheres as novel antigen delivery systems. *Int J Nanotechnol* 2013;**10**:870–90.
88. Xing L, Shi Q, Zheng K, Shen M, Ma J, Li F, et al. Ultrasound-mediated microbubble destruction (UMMD) facilitates the delivery of CA19-9 targeted and paclitaxel loaded mPEG-PLGA-PLL nanoparticles in pancreatic cancer. *Theranostics* 2016;**6**:1573–87.
89. Axelson H, Fredlund E, Ovenberger M, Landberg G, Pahlman S. Hypoxia-induced dedifferentiation of tumor cells—a mechanism behind heterogeneity and aggressiveness of solid tumors. *Semin Cell Dev Biol* 2005;**16**:554–63.

90. Vaupel P. Tumor microenvironmental physiology and its implications for radiation oncology. *Semin Radiat Oncol* 2004;**14**:198–206.
91. Riess JG. Oxygen carriers (“blood substitutes”)—raison d’être, chemistry, and some physiology. *Chem Rev* 2001;**101**:2797–920.
92. Castro CI, Briceno JC. Perfluorocarbon-based oxygen carriers: review of products and trials. *Artif Organs* 2010;**34**:622–34.
93. Ren H, Liu J, Li Y, Wang H, Ge S, Yuan A, et al. Oxygen self-enriched nanoparticles functionalized with erythrocyte membranes for long circulation and enhanced phototherapy. *Acta Biomater* 2017;**59**:269–82.
94. Gao M, Liang C, Song X, Chen Q, Jin Q, Wang C, et al. Erythrocyte-membrane-enveloped perfluorocarbon as nanoscale artificial red blood cells to relieve tumor hypoxia and enhance cancer radiotherapy. *Adv Mater* 2017;**29**:1701429.
95. Zhang Z, Qian H, Yang M, Li R, Hu J, Li L, et al. Gambogic acid-loaded biomimetic nanoparticles in colorectal cancer treatment. *Int J Nanomed* 2017;**12**:1593–605.
96. Gao L, Wang H, Nan L, Peng T, Sun L, Zhou J, et al. Erythrocyte membrane-wrapped pH sensitive polymeric nanoparticles for non-small cell lung cancer therapy. *Bioconj Chem* 2017;**28**:2591–8.
97. Guo Y, Wang D, Song Q, Wu T, Zhuang X, Bao Y, et al. Erythrocyte membrane-enveloped polymeric nanoparticles as nanovaccine for induction of antitumor immunity against melanoma. *ACS Nano* 2015;**9**:6918–33.
98. Hao R, Xing R, Xu Z, Hou Y, Gao S, Sun S. Synthesis, functionalization, and biomedical applications of multifunctional magnetic nanoparticles. *Adv Mater* 2010;**22**:2729–42.
99. Sharifi S, Seyednejad H, Laurent S, Atyabi F, Saei AA, Mahmoudi M. Superparamagnetic iron oxide nanoparticles for *in vivo* molecular and cellular imaging. *Contrast Media Mol Imaging* 2015;**10**:329–55.
100. Yoshida T, Sasayama T, Enpuku K. (Invited) Biological applications of magnetic nanoparticles for magnetic immunoassay and magnetic particle imaging. *ECS Trans* 2016;**75**:39–47.
101. Rao L, Bu LL, Xu JH, Cai B, Yu GT, Yu X, et al. Red blood cell membrane as a biomimetic nanocoating for prolonged circulation time and reduced accelerated blood clearance. *Small* 2015;**11**:6225–36.
102. Owens DR, Peppas NA. Opsonization, biodistribution, and pharmacokinetics of polymeric nanoparticles. *Int J Pharm* 2006;**307**:93–102.
103. Chu M, Shao Y, Peng J, Dai X, Li H, Wu Q, et al. Near-infrared laser light mediated cancer therapy by photothermal effect of Fe₃O₄ magnetic nanoparticles. *Biomaterials* 2013;**34**:4078–88.
104. Chen H, Burnett J, Zhang F, Zhang J, Paholak H, Sun D. Highly crystallized iron oxide nanoparticles as effective and biodegradable mediators for photothermal cancer therapy. *J Mater Chem B* 2014;**2**:757–65.
105. Shen S, Wang S, Zheng R, Zhu X, Jiang X, Fu D, et al. Magnetic nanoparticle clusters for photothermal therapy with near-infrared irradiation. *Biomaterials* 2015;**39**:67–74.
106. Ding H, Lv Y, Ni D, Wang J, Tian Z, Wei W, et al. Erythrocyte membrane-coated NIR-triggered biomimetic nanovectors with programmed delivery for photodynamic therapy of cancer. *Nanoscale* 2015;**7**:9806–15.
107. Zhou Y, Quan G, Wu Q, Zhang X, Niu B, Wu B, et al. Mesoporous silica nanoparticles for drug and gene delivery. *Acta Pharm Sin B* 2018;**8**:165–77.
108. Su J, Sun H, Meng Q, Zhang P, Yin Q, Li Y. Enhanced blood suspensibility and laser-activated tumor-specific drug release of theranostic mesoporous silica nanoparticles by functionalizing with erythrocyte membranes. *Theranostics* 2017;**7**:523–37.
109. Vernier PT, Levine ZA, Wu YH, Joubert V, Ziegler MJ, Mir LM, et al. Electroporating fields target oxidatively damaged areas in the cell membrane. *PLoS One* 2009;**4**:e7966.
110. Cheng L, Yang K, Li Y, Chen J, Wang C, Shao M, et al. Facile preparation of multifunctional upconversion nanoprobe for multimodal imaging and dual-targeted photothermal therapy. *Angew Chem Int Ed Engl* 2011;**50**:7385–90.
111. Yang Y, Zhao Q, Feng W, Li F. Luminescent chemodosimeters for bioimaging. *Chem Rev* 2013;**113**:192–270.
112. Yang D, Dai Y, Liu J, Zhou Y, Chen Y, Li C, et al. Ultra-small BaGdF₅-based upconversion nanoparticles as drug carriers and multimodal imaging probes. *Biomaterials* 2014;**35**:2011–23.
113. Rieffel J, Chen F, Kim J, Chen G, Shao W, Shao S, et al. Hexamodal imaging with porphyrin-phospholipid-coated upconversion nanoparticles. *Adv Mater* 2015;**27**:1785–90.
114. Chen Z, Liu Z, Li Z, Ju E, Gao N, Zhou L, et al. Upconversion nanoprobe for efficiently *in vitro* imaging reactive oxygen species and *in vivo* diagnosing rheumatoid arthritis. *Biomaterials* 2015;**39**:15–22.
115. Zhang F, Braun GB, Shi Y, Zhang Y, Sun X, Reich NO, et al. Fabrication of Ag@SiO₂@Y₂O₃:Er nanostructures for bioimaging: tuning of the upconversion fluorescence with silver nanoparticles. *J Am Chem Soc* 2010;**132**:2850–1.
116. Li J, Huang J, Ao Y, Li S, Miao Y, Yu Z, et al. Synergizing upconversion nanophotosensitizers with hyperbaric oxygen to remodel the extracellular matrix for enhanced photodynamic cancer therapy. *ACS Appl Mater Interfaces* 2018;**10**:22985–96.
117. Giljohann DA, Seferos DS, Daniel WL, Massich MD, Patel PC, Mirkin CA. Gold nanoparticles for biology and medicine. *Angew Chem Int Ed Engl* 2010;**49**:3280–94.
118. Dreaden EC, Alkilany AM, Huang X, Murphy CJ, El-Sayed MA. The golden age: gold nanoparticles for biomedicine. *Chem Soc Rev* 2012;**41**:2740–79.
119. Moon GD, Choi SW, Cai X, Li W, Cho EC, Jeong U, et al. A new theranostic system based on gold nanocages and phase-change materials with unique features for photoacoustic imaging and controlled release. *J Am Chem Soc* 2011;**133**:4762–5.
120. Pan L, Liu J, He Q, Shi J. MSN-mediated sequential vascular-to-cell nuclear-targeted drug delivery for efficient tumor regression. *Adv Mater* 2014;**26**:6742–8.
121. Farokhzad OC, Langer R. Nanomedicine: developing smarter therapeutic and diagnostic modalities. *Adv Drug Deliv Rev* 2006;**58**:1456–9.
122. Toth M, Sohai A, Fridman R. Assessment of gelatinases (MMP-2 and MMP-9) by gelatin zymography. *Methods Mol Biol* 2012;**878**:121–35.
123. Li LL, Xu JH, Qi GB, Zhao X, Yu F, Wang H. Core-shell supramolecular gelatin nanoparticles for adaptive and “on-demand” antibiotic delivery. *ACS Nano* 2014;**8**:4975–83.
124. Bose RJ, Paulmurugan R, Moon J, Lee SH, Park H. Cell membrane-coated nanocarriers: the emerging targeted delivery system for cancer theranostics. *Drug Discov Today* 2018;**23**:891–9.
125. Davis ME, Chen ZG, Shin DM. Nanoparticle therapeutics: an emerging treatment modality for cancer. *Nat Rev Drug Discov* 2008;**7**:771–82.
126. Peer D, Karp JM, Hong S, Farokhzad OC, Margalit R, Langer R. Nanocarriers as an emerging platform for cancer therapy. *Nat Nanotechnol* 2007;**2**:751–60.
127. Wagner V, Dullaart A, Bock AK, Zweck A. The emerging nanomedicine landscape. *Nat Biotechnol* 2006;**24**:1211–7.
128. Zhang L, Gu FX, Chan JM, Wang AZ, Langer RS, Farokhzad OC. Nanoparticles in medicine: therapeutic applications and developments. *Clin Pharmacol Ther* 2008;**83**:761–9.
129. Remant BKC, Thapa B, Xu P. pH and redox dual responsive nanoparticle for nuclear targeted drug delivery. *Mol Pharm* 2012;**9**:2719–29.
130. Bartczak D, Kanaras AG. Preparation of peptide-functionalized gold nanoparticles using one pot EDC/Sulfo-NHS coupling. *Langmuir* 2011;**27**:10119–23.
131. Chen T, I Ö, Yuan Q, Wang R, You M, Zhao Z, et al. One-step facile surface engineering of hydrophobic nanocrystals with designer molecular recognition. *J Am Chem Soc* 2012;**134**:13164–7.
132. Hu CM, Kaushal S, Tran Cao HS, Aryal S, Sartor M, Esener S, et al. Half-antibody functionalized lipid-polymer hybrid nanoparticles for targeted drug delivery to carcinoembryonic antigen presenting pancreatic cancer cells. *Mol Pharm* 2010;**7**:914–20.
133. Jin E, Zhang B, Sun X, Zhou Z, Ma X, Sun Q, et al. Acid-active cell-penetrating peptides for *in vivo* tumor-targeted drug delivery. *J Am Chem Soc* 2012;**135**:933–40.

134. Johnston AP, Kamphuis MM, Such GK, Scott AM, Nice EC, Heath JK, et al. Targeting cancer cells: controlling the binding and internalization of antibody-functionalized capsules. *ACS Nano* 2012;**6**:6667–74.
135. Wang J, Tian S, Petros RA, Napier ME, Desimone JM. The complex role of multivalency in nanoparticles targeting the transferrin receptor for cancer therapies. *J Am Chem Soc* 2010;**132**:11306–13.
136. Fang RH, Hu CM, Chen KN, Luk BT, Carpenter CW, Gao W, et al. Lipid-insertion enables targeting functionalization of erythrocyte membrane-cloaked nanoparticles. *Nanoscale* 2013;**5**:8884–8.
137. Rao L, Meng QF, Bu LL, Cai B, Huang Q, Sun ZJ, et al. Erythrocyte membrane-coated upconversion nanoparticles with minimal protein adsorption for enhanced tumor imaging. *ACS Appl Mater Interfaces* 2017;**9**:2159–68.
138. Chai Z, Hu X, Wei X, Zhan C, Lu L, Jiang K, et al. A facile approach to functionalizing cell membrane-coated nanoparticles with neurotoxin-derived peptide for brain-targeted drug delivery. *J Control Release* 2017;**264**:102–11.
139. Zhu DM, Xie W, Xiao YS, Suo M, Zan MH, Liao QQ, et al. Erythrocyte membrane-coated gold nanocages for targeted cancer photothermal and chemical therapy. *Nanotechnology* 2018;**29**:084002.
140. Fu Q, Lv P, Chen Z, Ni D, Zhang L, Yue H, et al. Programmed co-delivery of paclitaxel and doxorubicin boosted by camouflaging with erythrocyte membrane. *Nanoscale* 2015;**7**:4020–30.
141. Hsieh CC, Kang ST, Lin YH, Ho YJ, Wang CH, Yeh CK, et al. Biomimetic acoustically-responsive vesicles for theranostic applications. *Theranostics* 2015;**5**:1264–74.
142. Li R, He Y, Zhang S, Qin J, Wang J. Cell membrane-based nanoparticles: a new biomimetic platform for tumor diagnosis and treatment. *Acta Pharm Sin B* 2018;**8**:14–22.